

Gapped paramagnetic state in a frustrated spin- $\frac{1}{2}$ Heisenberg antiferromagnet on the cross-striped square lattice

P H Y Li^{1,2} and R F Bishop^{1,2}

¹ *School of Physics and Astronomy, Schuster Building, The University of Manchester, Manchester, M13 9PL, UK*

² *School of Physics and Astronomy, University of Minnesota, 116 Church Street SE, Minneapolis, Minnesota 55455, USA*

Abstract

We implement the coupled cluster method to very high orders of approximation to study the spin- $\frac{1}{2}$ J_1 - J_2 Heisenberg model on a cross-striped square lattice. Every nearest-neighbour pair of sites on the square lattice has an isotropic antiferromagnetic exchange bond of strength $J_1 > 0$, while the basic square plaquettes in alternate columns have either both or neither next-nearest-neighbour (diagonal) pairs of sites connected by an equivalent frustrating bond of strength $J_2 \equiv \alpha J_1 > 0$. By studying the magnetic order parameter (i.e., the average local on-site magnetization) in the range $0 \leq \alpha \leq 1$ of the frustration parameter we find that the quasiclassical antiferromagnetic Néel and (so-called) double Néel states form the stable ground-state phases in the respective regions $\alpha < \alpha_{1a}^c = 0.46(1)$ and $\alpha > \alpha_{1b}^c = 0.615(5)$. The double Néel state has Néel ($\cdots \uparrow\downarrow\uparrow\downarrow \cdots$) ordering along the (column) direction parallel to the stripes of squares with both or no J_2 bonds, and spins alternating in a pairwise ($\cdots \uparrow\uparrow\downarrow\downarrow\uparrow\uparrow\downarrow\downarrow \cdots$) fashion along the perpendicular (row) direction, so that the parallel pairs occur on squares with both J_2 bonds present. Further explicit calculations of both the triplet spin gap and the zero-field uniform transverse magnetic susceptibility provide compelling evidence that the ground-state phase over all or most of the intermediate regime $\alpha_{1a}^c < \alpha < \alpha_{1b}^c$ is a gapped state with no discernible long-range mag-

Email address: peggyhyli@gmail.com; raymond.bishop@manchester.ac.uk (P H Y Li^{1,2} and R F Bishop^{1,2})

netic order.

Keywords: gapped paramagnetic state, cross-stripped square lattice, J_1 - J_2 Heisenberg model, coupled cluster method

1. Introduction

Frustrated quantum magnets, in which competing types of interactions vie with one another, even at the classical level, to promote different forms of magnetic long-range order (LRO), provide notoriously difficult challenges for any computational many-body technique [1]. At the theoretical level the underlying spin-lattice models are of huge interest since their zero-temperature ($T = 0$) phase diagrams (in the space spanned by the parameters describing the interaction strengths of the competing interactions in the model Hamiltonian) often display a rich variety of phases with orderings that have no classical counterparts. The resulting quantum phase transitions provide a challenging theoretical and computational arena in which to describe accurately the physical properties of the models near their corresponding quantum critical points (QCPs) at which long-range many-body quantum entanglement, driven by frustration, is paramount [2]. At the same time such spin-lattice models are also of great interest experimentally, since they often mimic rather accurately the properties of a large variety of real materials.

Of particular interest in this respect are two-dimensional (2D) models. This is partly because the effects of quantum fluctuations are higher in systems with reduced dimensionality, and also because in recent years a large number of layered quasi-2D real magnetic materials have been synthesised in which the strengths of the intralayer magnetic interactions are much larger than those acting between layers. Furthermore, many such synthetic 2D spin-lattice systems are now increasingly being modelled rather accurately using the properties of suitable ultracold atoms trapped in 2D optical lattices. The great advantage of the latter is that in such experiments one can also tune the system so as effectively to vary the relative strengths of the competing interaction terms in the Hamiltonian. In this way one may attempt to sweep over any pertinent QCPs [3]. One role of the theorist in this endeavour is then to suggest suitably interesting models for the experimentalist to attempt to mimic.

One particularly interesting, and especially challenging, model in this respect is the J_1 - J_2 model on the 2D square lattice in which antiferromag-

netic (AFM) nearest-neighbour (NN) isotropic (XXX) Heisenberg interactions with exchange coupling strength parameter $J_1 > 0$ compete with next-nearest-neighbour (NNN) XXX Heisenberg interactions with respective strength parameter $J_2 > 0$. This archetypal model, which was introduced nearly 30 years ago in an attempt to describe the disappearance of AFM Néel LRO in the cuprate high-temperature superconductors [4–6], has since then received huge theoretical interest. In particular, many different theoretical and computational techniques have been used to study it (see, e.g., Refs. [7–39]). These include several very successful applications [12, 16, 18–20, 39] of the coupled cluster method (CCM).

Of comparable theoretical interest and equally challenging, but less studied, is the family of half-depleted square-lattice J_1 – J_2 models, in which half of the NNN J_2 bonds are removed in an ordered fashion. Two of the most interesting members of this class are the so-called anisotropic planar pyrochlore (or anisotropic checkerboard model) and the cross-striped square-lattice model, in both of which half of the basic square plaquettes formed from four NN J_1 bonds have both diagonal J_2 bonds retained (i.e., the filled squares) while the rest have neither (i.e., the empty squares). They differ in that, while in the former model the empty and filled squares alternate along both rows and columns of the square lattice, the latter comprises alternating columns (or, equivalently, rows) of filled and empty squares. While the anisotropic planar pyrochlore has been studied by a variety of methods in the past including the CCM (see, e.g., Refs. [40, 41] and references contained therein), the equally interesting cross-striped square-lattice model has, somewhat surprisingly, received only scant attention [42]. As a consequence we apply the CCM to it here in order to investigate further its $T = 0$ phase diagram. Our main finding will be to confirm that the spin- $\frac{1}{2}$ model has an intermediate paramagnetic state with no obvious magnetic LRO that lies between the two classical states with AFM order in the frustrated case where $J_1 > 0$ and $J_2 > 0$. Furthermore, we find compelling evidence that this intermediate state is gapped.

2. The model

We study the Hamiltonian

$$H = J_1 \sum_{\langle i,j \rangle} \mathbf{s}_i \cdot \mathbf{s}_j + J_2 \sum_{\langle\langle i,k \rangle\rangle'} \mathbf{s}_i \cdot \mathbf{s}_k, \quad (1)$$

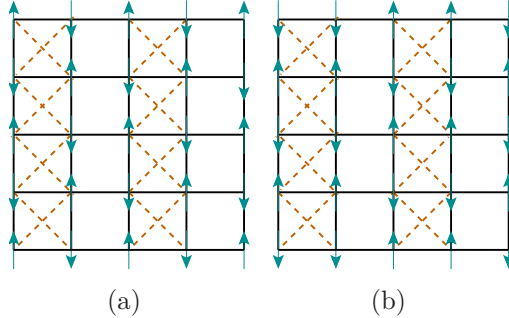


Figure 1: The J_1 - J_2 Heisenberg model on a cross-striped square lattice. The solid (black) lines are J_1 bonds and the dashed (brown) lines are J_2 bonds. The (cyan) arrows represent the relative spin directions in: (a) the Néel state, and (b) the double Néel (DN) state.

where the operators $\mathbf{s}_i \equiv (s_i^x, s_i^y, s_i^z)$ are spin- s SU(2) operators on each of the $N \rightarrow \infty$ sites i of a 2D square lattice. We consider here the extreme quantum case $s = \frac{1}{2}$. The sum over $\langle i, j \rangle$ and $\langle\langle i, k \rangle\rangle'$ run respectively over all distinct NN bonds and over half of the distinct NNN (diagonal) bonds in the cross-striped pattern shown in Fig. 1. We are interested here in investigating the $T = 0$ phase diagram of the spin- $\frac{1}{2}$ model when both bonds are AFM in nature (i.e., $J_1 > 0$, $J_2 \equiv \alpha J_1 > 0$), and hence act to frustrate one another.

The phase diagram for the model in the classical ($s \rightarrow \infty$) limit has been discussed in detail in Ref. [42]. In our region of interest there are two stable AFM ground-state (GS) phases, shown in Figs. 1(a) and 1(b) respectively, separated by a first-order transition at the critical point $\alpha^{\text{cl}} = \frac{1}{2}$. For values $\alpha < \alpha^{\text{cl}}$ of the frustration parameter the classical system has Néel LRO, as shown in Fig. 1(a). However, for values $\alpha > \alpha^{\text{cl}}$, another collinear AFM state, the so-called double Néel (DN) state shown in Fig. 1(b), forms the stable GS phase. It has AFM Néel ordering along the direction parallel to the stripes of filled squares (viz., along columns in Fig. 1), together with spins alternating in a pairwise fashion along the perpendicular direction. Thus NN spins are parallel on filled squares and antiparallel on empty squares in the row direction in Fig. 1(b).

In the present study we will employ both of these classical GS AFM phases as reference states. Neither of them are eigenstates of the quantum Hamiltonian for the case $s = \frac{1}{2}$ under study, but we will use the CCM as

a systematic tool to incorporate the quantum many-body correlations on top of them within a controlled approximation hierarchy that asymptotically becomes exact as one approaches the infinite-order limit. We will implement the method computationally to high orders of approximation and then use well-known extrapolation schemes to calculate various physical quantities for the model, including the magnetic order parameter, the zero-field transverse magnetic susceptibility and the triplet spin gap.

In order to calculate the susceptibility we place the system in a transverse uniform magnetic field $\mathbf{h} = h\hat{x}_s$, where \hat{x}_s is a unit vector in the spin-space x -direction. The Hamiltonian $H \equiv H(h = 0)$ of Eq. (1) then becomes $H(h) = H(0) - h \sum_{k=1}^N s_k^x$, in units where the gyromagnetic ratio $g\mu_B/\hbar = 1$. The spins, previously aligned as shown in Figs. 1(a) and 1(b), respectively, in the Néel and DN states, now cant at an angle $\theta = \theta(h)$ with respect to their zero-field configurations along the spin-space z -direction. These canted states are used as our CCM reference states in the case of an applied external magnetic field, and θ is calculated in practice [43] so as to minimize the energy expectation value $E(h)$ for a given value of h at each level of CCM approximation discussed below. We define the (uniform) transverse magnetic susceptibility as usual by $\chi(h) = -N^{-1}d^2E/dh^2$, and its zero-field limit as $\chi \equiv \chi(0)$. It is simple to calculate $\theta(h)$ and hence χ for the two classical ($s \rightarrow \infty$) AFM states in Fig. 1, thereby obtaining the classical result for the model,

$$J_1\chi^{\text{cl}} = \begin{cases} \frac{1}{8}; & \alpha \leq \frac{1}{2}, \\ \frac{1}{2}(3 + 2\alpha)^{-1}; & \alpha \geq \frac{1}{2}, \end{cases} \quad (2)$$

where $\alpha \equiv J_2/J_1$ is the frustration parameter, and $J_1 > 0$.

3. The coupled cluster method

The CCM [44–47] is one of the most flexible and most accurate techniques of microscopic quantum many-body theory. It is both size-consistent and size-extensive, and thereby provides results in the infinite-lattice ($N \rightarrow \infty$) limit at every level of approximation. The quantum correlations are expressed in a suitably exponentiated form, which is the hallmark of the CCM, on top of suitably chosen model (or reference) states (and see, e.g., Refs. [12, 46–48]). We use here the Néel and DN states shown in Fig. 1, together with their canted versions for the calculation of χ . For the current $s = \frac{1}{2}$

model we also use the extensively used and very well-tested localized lattice-animal-based subsystem (LSUB m) truncation hierarchy of approximation [46–48]. At the corresponding m th level of approximation one retains all multispin correlations in the CCM correlation operators that are defined over all distinct locales (or lattice animals) on the lattice that comprise m or fewer contiguous sites (i.e., those in which every site is NN to at least one other). Very importantly, the method preserves both the Goldstone linked-cluster theorem and the Hellmann-Feynman theorem at every LSUB m level of approximation. The techniques involved in deriving and solving the large and inherently nonlinear sets of coupled CCM equations at high LSUB m orders have been extensively discussed in the literature (see, eg., Refs. [12, 46–48]), and will not be repeated here.

Space- and point-group symmetries of both the Hamiltonian and the CCM reference state, together with any conservation laws, are used to reduce the set of independent spin configurations retained in the CCM LSUB m correlation operators to a minimal number, $N_f(m)$. Nevertheless, N_f increases rapidly as the truncation index m is increased. Accordingly, one needs both considerable supercomputing resources and massive parallelization for the higher-order calculations [46, 49]. For the present spin- $\frac{1}{2}$ model we are able to perform LSUB m calculations for $m \leq 10$ for both the ground and lowest-lying spin-triplet excited states based on either the Néel or DN AFM states as CCM model states, and using the cross-stripped square-lattice geometry in which all pairs of sites connected by either J_1 or J_2 bonds are considered as NN pairs for the purposes of contiguity contained in the selection of LSUB m multispin clusters. For example, for the GS results (in the absence of any external magnetic field) at the LSUB10 level, we have $N_f = 768\,250$ (853 453) using the Néel (DN) reference states. Similarly, for the LSUB10 calculation of the triplet spin gap Δ , we have $N_f = 1\,400\,161$ (1 500 377) using the Néel (DN) reference states. Due to the much reduced symmetries of the respective canted states in the presence of an external magnetic field, we are only able to perform LSUB m calculations for χ with $m \leq 8$. Thus, we have $N_f = 203\,508$ (203 445) at the LSUB8 level for calculations based on the canted Néel (DN) reference states.

The *only* approximation made in our CCM calculations comes in the final step of extrapolation to the exact $m \rightarrow \infty$ limit. Although no exact such schemes are known, by now a great deal of experience has been accumulated from an extremely large number of successful applications of the CCM to many spin-lattice models (see, e.g., [16, 18–20, 39–43, 46–48] and references

contained therein). Thus, for example, for the LSUB m approximation $M(m)$ of the magnetic order parameter (viz., the average local on-site magnetization) M we use the scheme

$$M(m) = \mu_0 + \mu_1 m^{-1/2} + \mu_2 m^{-3/2}, \quad (3)$$

which has been found to be appropriate for highly frustrated systems, particularly in the vicinity of a QCP, to extract the extrapolated value μ_0 for M . Similarly, very well-tested schemes for the LSUB m approximants $\Delta(m)$ and $\chi(m)$ of the respective triplet spin gap and the zero-field transverse magnetic susceptibility χ are

$$\Delta(m) = d_0 + d_1 m^{-1} + d_2 m^{-2}, \quad (4)$$

and

$$\chi(m) = x_0 + x_1 m^{-1} + x_2 m^{-2}, \quad (5)$$

and we utilize both schemes here to extract the extrapolated values d_0 and x_0 , respectively.

4. Results and Discussion

We first present in Fig. 2 our CCM results for the GS magnetic order parameter M of the spin- $\frac{1}{2}$ J_1 - J_2 Heisenberg antiferromagnet on a cross-stripped square lattice. Results at LSUB m levels of approximation with $m \leq 10$ are shown, based on both the quasiclassical Néel and DN states illustrated in Figs. 1(a) and 1(b), respectively, used as CCM model states. We also display in Fig. 2 the corresponding ($m \rightarrow \infty$) LSUB ∞ extrapolations obtained from the use of Eq. (3). In order to illustrate the robustness of the extrapolation, which we reiterate is the *sole* approximation that we make, we show explicitly for both AFM phases three separate such extrapolations, based on the respective LSUB m data sets $m = \{2, 6, 10\}$, $m = \{4, 6, 8\}$ and $m = \{4, 6, 8, 10\}$, each used separately as input to Eq. (3).

It is clear from Fig. 2 that both quasiclassical GS phases lose their stability in a regime around the point $\alpha^{\text{cl}} = \frac{1}{2}$ where the classical ($s \rightarrow \infty$) version of the model shows a phase transition between the two AFM phases. Indeed, the extrapolations show clear and consistent evidence for a phase in the intermediate range $\alpha_{1a}^c < \alpha < \alpha_{1b}^c$ with no classical counterpart. For $\alpha < \alpha_{1a}^c$ the system has a GS phase with Néel AFM LRO, whereas for $\alpha > \alpha_{1b}^c$ the GS phase has DN AFM LRO, with $\alpha_{1a}^c < \alpha^{\text{cl}} < \alpha_{1b}^c$.

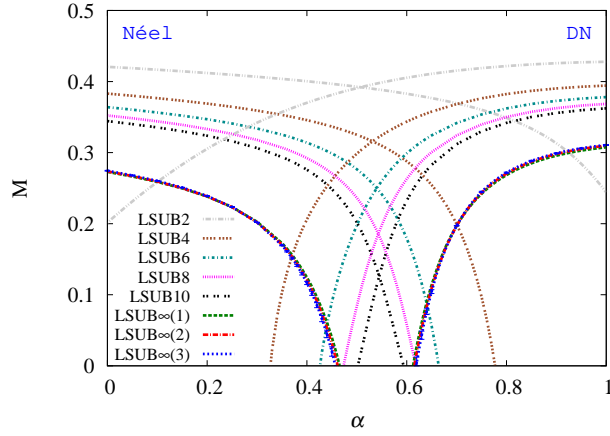


Figure 2: CCM results for the GS magnetic order parameter M as a function of the frustration parameter $\alpha \equiv J_2/J_1$ for the spin- $\frac{1}{2}$ J_1 - J_2 model on a cross-stripped square lattice, with $J_1 > 0$. Results are shown based on both the quasiclassical Néel (left curves) and DN (right curves) AFM states used as the CCM model state, in LSUB m approximations with $m = 2, 4, 6, 8, 10$. Also shown are two corresponding sets of three LSUB $\infty(i)$ extrapolations, each based on Eq. (3) but using as input the separate respective data sets with $m = \{2, 6, 10\}$ for $i = 1$, $m = \{4, 6, 8\}$ for $i = 2$ and $m = \{4, 6, 8, 10\}$ for $i = 3$.

In order to fit extrapolation schemes of the forms of Eqs. (3)–(5) that contain three fitting parameters it is clearly preferable to use input data sets comprising greater than three values. In this way we can also calculate the error bars associated with the least-squares fits. These are shown, for example, in the $\text{LSUB}\infty(3)$ extrapolation shown in Fig. 2, which is based on the $\text{LSUB}m$ input data set with $m = \{4, 6, 8, 10\}$ for the calculated values of $M(m)$ at each value of α . The errors associated with the fit are generally extremely small, indicating its overall accuracy, although they do become somewhat larger in the vicinity of the QCPs at α_{1a}^c and α_{1b}^c where M becomes small. The numerical values of the two phase transition points obtained from the $\text{LSUB}\infty(3)$ extrapolation are $\alpha_{1a}^c = 0.457$ and $\alpha_{1b}^c = 0.619$.

As a further demonstration of the extremely robust nature of the extrapolation procedure we also show in Fig. 2 two other fits using only three input data points, namely $\text{LSUB}\infty(1)$ using the $\text{LSUB}m$ input data set with $m = \{2, 6, 10\}$ and $\text{LSUB}\infty(2)$ with $m = \{4, 6, 8\}$. Both are in very close agreement with the intrinsically more accurate $\text{LSUB}\infty(3)$ fit that uses the four input data points $m = \{4, 6, 8, 10\}$, even the $\text{LSUB}\infty(1)$ fit that includes the lowest-order $\text{LSUB}m$ approximant with $m = 2$. The corresponding values obtained for the two phase transition points are $\alpha_{1a}^c = 0.466$ and $\alpha_{1b}^c = 0.613$ from the $\text{LSUB}\infty(1)$ fit, and $\alpha_{1a}^c = 0.462$ and $\alpha_{1b}^c = 0.616$ from the $\text{LSUB}\infty(2)$ fit. A more detailed sensitivity analysis using these (and other similar such) fits yields our best values, $\alpha_{1a}^c = 0.46(1)$ and $\alpha_{1b}^c = 0.615(5)$, as obtained from our CCM calculations for the vanishing of the magnetic order parameter M in the Néel and DN AFM phases, respectively.

The question that now immediately arises is what is the nature of the intermediate phase without magnetic LRO? Perhaps the simplest but certainly not the only possible scenario in this case for the loss of LRO is that the spin-spin correlation function between two spins at lattice sites k and l decays exponentially as a function of the distance $|\mathbf{r}_k - \mathbf{r}_l|$ between them on the lattice,

$$|\langle \mathbf{s}_k \cdot \mathbf{s}_l \rangle| \propto \exp(-i|\mathbf{r}_k - \mathbf{r}_l|/\xi). \quad (6)$$

A system in such a phase with a finite correlation length ξ behaves just as a finite system of comparable linear size, and hence the quantized energy levels are discrete. Accordingly, such a system will have no low-energy excitations. Its ground state will be a spin singlet, just as we have assumed in our CCM calculations for the two quasiclassical AFM states, and the lowest-lying triplet excited state will lie at a finite energy, $\Delta > 0$, above the ground state.

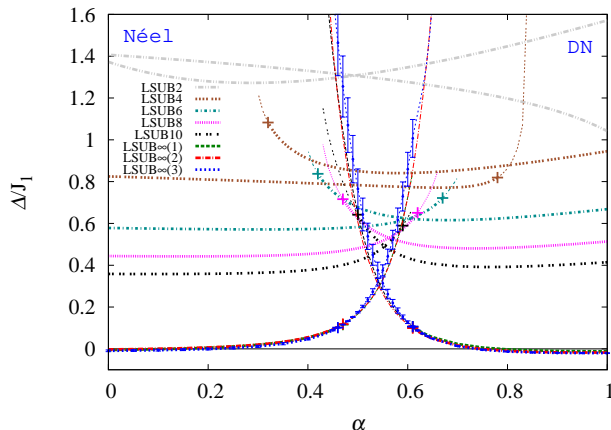


Figure 3: CCM results for the triplet spin gap Δ (in units of J_1) as a function of the frustration parameter $\alpha \equiv J_2/J_1$ for the spin- $\frac{1}{2}$ J_1 - J_2 model on a cross-striped square lattice, with $J_1 > 0$. Results are shown based on both the quasiclassical Néel (left curves) and DN (right curves) AFM states with a single spin-flip used as the CCM model state, in LSUB m approximations with $m = 2, 4, 6, 8, 10$. Also shown are two corresponding sets of three LSUB $\infty(i)$ extrapolations, each based on Eq. (4) but using as input the separate respective data sets with $m = \{2, 6, 10\}$ for $i = 1$, $m = \{4, 6, 8\}$ for $i = 2$ and $m = \{4, 6, 8, 10\}$ for $i = 3$. The points where the respective CCM solution has $M \rightarrow 0$ are shown by plus (+) symbols, and those unphysical portions of the curves beyond these points, where $M < 0$, are indicated by thinner lines.

In order to calculate the triplet spin gap Δ we now perform excited-state CCM calculations based on spin-triplet model states obtained from the two quasiclassical AFM states (i.e., the Néel and DN states) by flipping a single spin- $\frac{1}{2}$ particle.

We show in Fig. 3 our LSUB m results for the triplet spin gap Δ with $m \leq 10$ based on both the Néel and DN quasiclassical states with a single spin-flip, used separately as CCM model states. We also display three LSUB $\infty(i)$ extrapolations, each using the fitting scheme of Eq. (4) and with the same three different input data sets as used in Fig. 2 for M . For the Néel curves we first solve the CCM equations for the unfrustrated case $\alpha = 0$ to find the stable physical solution at each LSUB m order. Each such LSUB m solution is then tracked, as the frustration parameter α is incremented in small steps, out to the point where the solution terminates. The termination points for the excited-state equations can be seen from Fig. 3 to decrease monotonically as

the termination order m increases. They are just the analogues of those also typically found in the GS CCM equations. They are simply manifestations of the corresponding QCP in the system at which magnetic LRO, of the form implicit in the particular model state being used, melts, as have been seen and well discussed in many previous applications (see, e.g., Refs. [19, 40–42, 47] and references cited therein). As is commonly seen, each $\text{LSUB}m$ Néel solution terminates at a greater value of α than the exact ($\text{LSUB}\infty$) value α_{1a}^c . Hence, we are able to consider values for α that are appreciably beyond the actual transition at α_{1a}^c into the quantum paramagnetic phase. A similar situation also occurs on the other side of the transition, where we now track each $\text{LSUB}m$ solution based on the DN model state from high values of α down to a lower termination point. Again, as seen from Fig. 3, we are able to enter the region below the corresponding QCP at α_{1b}^c for all finite values of the $\text{LSUB}m$ truncation index m .

Clearly, parts of those regions beyond the respective QCPs that we may enter with our $\text{LSUB}m$ solutions based on particular model states are likely to be unphysical in the sense that the corresponding values for the order parameter M become negative. For both the individual $\text{LSUB}m$ solutions and the $\text{LSUB}\infty$ extrapolations we mark on the curves by plus (+) symbols the points where $M \rightarrow 0$, as determined from the corresponding curves in Fig. 2. The unphysical regions of the curves beyond these points where $M < 0$ are shown in Fig. 3 by thinner curves than the respective physical regions where $M > 0$, which are shown as thicker.

By comparing the three different $\text{LSUB}\infty(i)$ curves shown in Fig. 3 we see once again how extremely robust is our extrapolation procedure for Δ . The least-squares-fit error bars shown on the $\text{LSUB}\infty(3)$ extrapolation are also again very small, except deep in the unphysical ($M < 0$) region for both the Néel and DN curves beyond their totally unphysical crossing point. The extrapolated results clearly show that for values of α appreciably below α_{1a}^c on the Néel side and above α_{1b}^c on the DN side, the value of Δ is zero within extremely small errors. This is a very good independent check on our extrapolation procedure since in both regimes we have magnetic LRO, and the consequent low-energy magnon states (i.e., the soft Goldstone modes) are gapless. By contrast, in the intermediate regime, the GS phase clearly has a non-vanishing spin-triplet gap from our results. While the plus (+) symbols on the extrapolated curves, which mark our corresponding estimates for the two QCPs at α_{1a}^c and α_{1b}^c do not precisely lie on the $\Delta = 0$ axis and mark the points beyond which Δ becomes nonzero, the shapes of the curves in

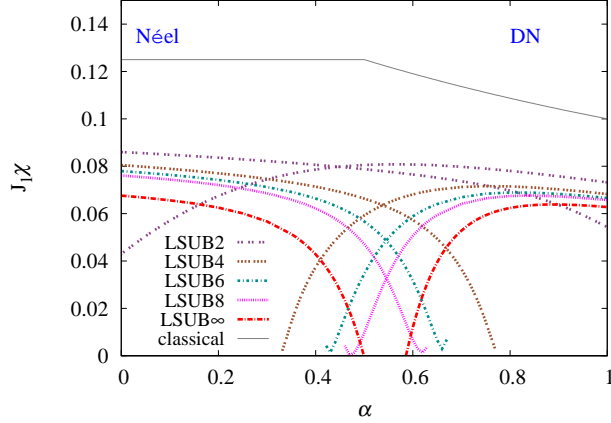


Figure 4: CCM results for the zero-field transverse magnetic susceptibility χ (in units of J_1^{-1} , and where the gyromagnetic ratio $g\mu_B/\hbar = 1$) as a function of the frustration parameter $\alpha \equiv J_2/J_1$, for the spin- $\frac{1}{2}$ J_1 - J_2 model on a cross-striped square lattice, with $J_1 > 0$. Results are shown based on both the canted quasiclassical Néel (left curves) and DN (right curves) AFM states as the CCM model states, in LSUB m approximations with $m = 2, 4, 6, 8$. Also shown are the extrapolation based on Eq. (5) and the data set with $m = \{4, 6, 8\}$ as input and, for comparison, the corresponding classical result of Eq. (2).

this region clearly militates against using the results for Δ to give accurate determinations of the critical values. Nevertheless, our results for Δ are in good agreement with those for M , and provide strong preliminary evidence that over the entire intermediate range $\alpha_{1a}^c < \alpha < \alpha_{1b}^c$ the GS phase is gapped.

In order both to corroborate these findings and to confirm the critical values of the frustration parameter it is now convenient to calculate the zero-energy (uniform) transverse magnetic susceptibility χ . Unlike for a system with magnetic LRO, a gapped system has no access to the low-energy excitations that make the susceptibility to an external magnetic field nonzero as the field becomes vanishingly small. Thus, at $T = 0$, a gapped system has $\chi = 0$ [50, 51]. In Fig. 4 we show our LSUB m results for χ based on both the canted Néel and DN states as CCM model states. As discussed previously, due to the reduced symmetries of those states compared to their zero-field counterparts, we can only perform LSUB m calculations now with $m \leq 8$. Accordingly, in Fig. 4, we only now show a single LSUB ∞ extrapolation based on the scheme of Eq. (5) and the data set with $m = \{4, 6, 8\}$ as input.

For both magnetically ordered phases the spin- $\frac{1}{2}$ system has an appreciably lower value of χ for a given value of α than its classical ($s \rightarrow \infty$) counterpart, as may be clearly seen from Fig. 4. More interestingly, each of the LSUB m curves with $m > 2$ approaches zero very closely at an upper (lower) critical value of α for the Néel (DN) case. Remarkably, in every case these critical values where $\chi(m) \rightarrow 0$ are identical (to within ± 0.01) to the corresponding LSUB m values where $M(m) \rightarrow 0$. Unlike for the case of Δ where there exists an appreciable unphysical regime where real solutions still exist beyond the points where $M(m) \rightarrow 0$, in the case of $\chi(m)$ the solutions terminate very rapidly after the points where $\chi(m) \rightarrow 0$, with the values increasing to become positive and nonzero again in these small regions. This behaviour is particularly clearly seen in Fig. 4 for the two sets of higher-order LSUB m curves with $m = 6, 8$.

The above behaviour, particularly the very close agreement for the critical values for α at which corresponding LSUB m values of $M(m)$ and $\chi(m)$ vanish, provides compelling evidence that the GS phase with no magnetic LRO, lying between the Néel and DN phases, is gapped everywhere. Nevertheless, the QCPs obtained from the LSUB ∞ curves for χ shown in Fig. 4, namely $\alpha_{1a}^c = 0.50$ and $\alpha_{1b}^c = 0.59$, are slightly different from our estimates $\alpha_{1a}^c = 0.46(1)$ and $\alpha_{1b}^c = 0.615(5)$ obtained from M . In the absence of a comparable sensitivity analysis of our results for χ , due to being restricted to performing LSUB m calculations with $m \leq 8$ in this case, it is difficult to say with complete authority whether the small discrepancies in the values obtained for the QCPs from M and χ are significant. Given the very close agreements, however, obtained at the individual LSUB m levels with $m \leq 8$, it seems most likely that the difference at the extrapolated levels is wholly within the unknown errors of the extrapolation for χ . Nevertheless, we cannot entirely rule out the possibility that the region intermediate between the magnetically ordered phases contains both a gapped phase within an inner region determined from the vanishing of χ on both sides and one or more gapless phases outside this region but still inside the region determined from the vanishing of the order parameter M for the two quasiclassical phases.

5. Conclusions

We have found that the single critical point at $\alpha^{\text{cl}} = \frac{1}{2}$ in the classical J_1 - J_2 model on the cross-stripped square lattice, which separates two different (viz., Néel and DN) states with AFM LRO, is split by quantum fluctuations

in the spin- $\frac{1}{2}$ version of the model into two QCPs at $\alpha_{1a}^c = 0.46(1)$ and $\alpha_{1b}^c = 0.615(5)$, at which the respective quasiclassical forms of magnetic LRO vanish. Further calculations of the triplet spin gap and the zero-field transverse magnetic susceptibility have provided convincing evidence that over most (and, most likely, all) of the intermediate range $\alpha_{1a}^c < \alpha < \alpha_{1b}^c$ the stable GS phase is a gapped state without any discernible magnetic LRO. This finding is in complete agreement with earlier work [42] on the spin- $\frac{1}{2}$ model that gave evidence of an intermediate state with plaquette valence-bond crystalline order.

Since the sole approximation made in our CCM calculations is the extrapolation of our series of LSUB m approximants to the exact $m \rightarrow \infty$ limit, and since we have been able to implement the method here to very high orders (viz., with $m \leq 10$), our results are inherently more accurate than can be attained in most alternative treatments. Furthermore, since the CCM, unlike most other methods, explicitly preserves the Hellmann-Feynman theorem at all levels of approximation, our results for the magnetic order parameter M and the zero-field transverse magnetic susceptibility χ , for example, are thus entirely compatible with each other at all LSUB m levels. This fact, together with our explicit LSUB m sets of results for M and χ , shown in Figs. 2 and 4 respectively, strengthens our belief that over the entire range $\alpha_{1a}^c < \alpha < \alpha_{1b}^c$ the stable GS phase is gapped. Nevertheless, even with these compelling arguments, we cannot entirely rule out the presence of very narrow regimes near one or both QCPs, α_{1a}^c and α_{1b}^c , at which quasiclassical AFM LRO vanishes, in which the GS phase is gapless. However, if they do exist, their extent in the parameter α is, undoubtedly, limited to a small part of the intermediate regime.

ACKNOWLEDGMENT

We thank the University of Minnesota Supercomputing Institute for the grant of supercomputing facilities. One of us (RFB) acknowledges the Leverhulme Trust (United Kingdom) for the award of an Emeritus Fellowship (EM-2015-007).

References

- [1] U. Schollwöck, J. Richter, D. J. J. Farnell, R. F. Bishop (Eds.), Quantum Magnetism, Vol. 645 of Lecture Notes in Physics, Springer-Verlag, Berlin, 2004.

- [2] S. Sachdev, Quantum Phase Transitions, 2nd Edition, Cambridge University Press, Cambridge, UK, 2011.
- [3] S. Sachdev, Quantum magnetism and criticality, Nat. Phys. 4 (2008) 173–185.
- [4] M. Inui, S. Doniach, M. Gabay, Doping dependence of antiferromagnetic correlations in high-temperature superconductors, Phys. Rev. B 38 (1988) 6631.
- [5] P. Chandra, B. Douçot, Possible spin-liquid state at large s for the frustrated square Heisenberg lattice, Phys. Rev. B 38 (1988) 9335.
- [6] E. Dagotto, A. Moreo, Phase diagram of the frustrated spin- $\frac{1}{2}$ Heisenberg antiferromagnet in two dimensions, Phys. Rev. Lett. 63 (1989) 2148.
- [7] H. J. Schulz, T. A. L. Ziman, Finite-size scaling for the two-dimensional frustrated quantum Heisenberg antiferromagnet, Europhys. Lett. 18 (1992) 355.
- [8] H. J. Schulz, T. A. L. Ziman, D. Poilblanc, Magnetic order and disorder in the frustrated quantum Heisenberg antiferromagnet in two dimensions, J. Phys. I France 6 (1996) 675.
- [9] J. Richter, Zero-temperature magnetic ordering in the inhomogeneously frustrated quantum Heisenberg antiferromagnet on a square lattice, Phys. Rev. B 47 (1993) 5794.
- [10] J. Richter, N. B. Ivanov, K. Retzlaff, On the violation of Marshall-Peierls sign rule in the frustrated J_1 - J_2 Heisenberg antiferromagnet, Europhys. Lett. 25 (1994) 545.
- [11] M. E. Zhitomirsky, K. Ueda, Valence-bond crystal phase of a frustrated spin- $\frac{1}{2}$ square-lattice antiferromagnet, Phys. Rev. B 54 (1996) 9007.
- [12] R. F. Bishop, D. J. J. Farnell, J. B. Parkinson, Phase transitions in the spin-half J_1 - J_2 model, Phys. Rev. B 58 (1998) 6394.
- [13] R. R. P. Singh, Z. Weihong, C. J. Hamer, J. Oitmaa, Dimer order with striped correlations in the J_1 - J_2 Heisenberg model, Phys. Rev. B 60 (1999) 7278.

- [14] L. Capriotti, F. Becca, A. Parola, S. Sorella, Resonating valence bond wave functions for strongly frustrated spin systems, Phys. Rev. Lett. 87 (2001) 097201.
- [15] J. Sirker, Z. Weihong, O. P. Sushkov, J. Oitmaa, J_1 - J_2 model: First-order phase transition versus deconfinement of spinons, Phys. Rev. B 73 (2006) 184420.
- [16] D. Schmalfuß, R. Darradi, J. Richter, J. Schulenburg, D. Ihle, Quantum J_1 - J_2 antiferromagnet on a stacked square lattice: Influence of the interlayer coupling on the ground-state magnetic ordering, Phys. Rev. Lett. 97 (2006) 157201.
- [17] M. Mambrini, A. Läuchli, D. Poilblanc, F. Mila, Plaquette valence-bond crystal in the frustrated Heisenberg quantum antiferromagnet on the square lattice, Phys. Rev. B 74 (2006) 144422.
- [18] R. F. Bishop, P. H. Y. Li, R. Darradi, J. Richter, The quantum J_1 - J'_1 - J_2 spin-1/2 Heisenberg model: influence of the interchain coupling on the ground-state magnetic ordering in two dimensions, J. Phys.: Condens. Matter 20 (2008) 255251.
- [19] R. F. Bishop, P. H. Y. Li, R. Darradi, J. Schulenburg, J. Richter, Effect of anisotropy on the ground-state magnetic ordering of the spin-half quantum J_1^{XXZ} - J_2^{XXZ} model on the square lattice, Phys. Rev. B 78 (2008) 054412.
- [20] R. Darradi, O. Derzhko, R. Zinke, J. Schulenburg, S. E. Krüger, J. Richter, Ground state phases of the spin-1/2 J_1 - J_2 Heisenberg antiferromagnet on the square lattice: A high-order coupled cluster treatment, Phys. Rev. B 78 (2008) 214415.
- [21] V. Murg, F. Verstraete, J. I. Cirac, Exploring frustrated spin systems using projected entangled pair states, Phys. Rev. B 79 (2009) 195119.
- [22] J. Richter, J. Schulenburg, The spin-1/2 J_1 - J_2 Heisenberg antiferromagnet on the square lattice: Exact diagonalization for $n = 40$ spins, Eur. Phys. J. B 73 (2010) 117.

- [23] J. Reuther, P. Wölfle, J_1 - J_2 frustrated two-dimensional Heisenberg model: Random phase approximation and functional renormalization group, Phys. Rev. B 81 (2010) 144410.
- [24] J.-F. Yu, Y.-J. Kao, Spin- $\frac{1}{2}$ J_1 - J_2 Heisenberg antiferromagnet on a square lattice: A plaquette renormalized tensor network study, Phys. Rev. B 85 (2012) 094407.
- [25] H.-C. Jiang, H. Yao, L. Balents, Spin liquid ground state of the spin- $\frac{1}{2}$ square J_1 - J_2 Heisenberg model, Phys. Rev. B 86 (2012) 024424.
- [26] F. Mezzacapo, Ground-state phase diagram of the quantum J_1 - J_2 model on the square lattice, Phys. Rev. B 86 (2012) 045115.
- [27] T. Li, F. Becca, W. Hu, S. Sorella, Gapped spin-liquid phase in the J_1 - J_2 Heisenberg model by a bosonic resonating valence-bond ansatz, Phys. Rev. B 86 (2012) 075111.
- [28] L. Wang, D. Poilblanc, Z.-C. Gu, X.-G. Wen, F. Verstraete, Constructing a gapless spin-liquid state for the spin-1/2 J_1 - J_2 Heisenberg model on a square lattice, Phys. Rev. Lett. 111 (2013) 037202.
- [29] W.-J. Hu, F. Becca, A. Parola, S. Sorella, Direct evidence for a gapless z_2 spin liquid by frustrating Néel antiferromagnetism, Phys. Rev. B 88 (2013) 060402(R).
- [30] X. Zhang, K. S. D. Beach, Resonating valence bond trial wave functions with both static and dynamically determined Marshall sign structure, Phys. Rev. B 87 (2013) 094420.
- [31] S.-S. Gong, W. Zhu, D. N. Sheng, O. I. Motrunich, M. P. A. Fisher, Plaquette ordered phase and quantum phase diagram in the spin- $\frac{1}{2}$ J_1 - J_2 square Heisenberg model, Phys. Rev. Lett. 113 (2014) 027201.
- [32] R. L. Doretto, Plaquette valence-bond solid in the square-lattice j_1 - j_2 antiferromagnet Heisenberg model: A bond operator approach, Phys. Rev. B 89 (2014) 104415.
- [33] Y. Qi, Z.-C. Gu, Continuous phase transition from Néel state to Z_2 spin-liquid state on a square lattice, Phys. Rev. B 89 (2014) 235122.

- [34] A. Metavitsiadis, D. Sellmann, S. Eggert, Spin-liquid versus dimer phases in an anisotropic J_1 - J_2 frustrated square antiferromagnet, *Phys. Rev. B* 89 (2014) 241104(R).
- [35] Y.-Z. Ren, N.-H. Tong, X.-C. Xie, Cluster mean-field theory study of J_1 - J_2 Heisenberg model on a square lattice, *J. Phys.: Condens. Matter* 26 (2014) 115601.
- [36] L. Wang, Correlated valence bond state and its study of the spin-1/2 J_1 - J_2 antiferromagnetic Heisenberg model on a square lattice, arXiv:1402.3564 (2014).
- [37] C.-P. Chou, H.-Y. Chen, Simulating a two-dimensional frustrated spin system with fermionic resonating-valence-bond states, *Phys. Rev. B* 90 (2014) 041106(R).
- [38] S. Morita, R. Kaneko, M. Imada, Quantum spin liquid in spin-1/2 J_1 - J_2 Heisenberg model on square lattice: Many-variable variational Monte Carlo study combined with quantum-number projections, *J. Phys. Soc. Jpn.* 84 (2015) 024720.
- [39] J. Richter, R. Zinke, D. J. J. Farnell, The spin-1/2 square-lattice J_1 - J_2 model: the spin-gap issue, *Eur. Phys. J. B* 88 (2015) 2.
- [40] R. F. Bishop, P. H. Y. Li, D. J. J. Farnell, J. Richter, C. E. Campbell, Frustrated Heisenberg antiferromagnet on the checkerboard lattice: J_1 - J_2 model, *Phys. Rev. B* 85 (2012) 205122.
- [41] P. H. Y. Li, R. F. Bishop, Ground-state phase structure of the spin- $\frac{1}{2}$ anisotropic planar pyrochlore, *J. Phys.: Condens. Matter* 27 (2015) 386002.
- [42] R. F. Bishop, P. H. Y. Li, C. E. Campbell, Spin- $\frac{1}{2}$ J_1 - J_2 Heisenberg model on a cross-stripped square lattice, *Phys. Rev. B* 88 (2013) 214418.
- [43] D. J. J. Farnell, R. Zinke, J. Schulenburg, J. Richter, High-order coupled cluster method study of frustrated and unfrustrated quantum magnets in external magnetic fields, *J. Phys.: Condens. Matter* 21 (2009) 406002.
- [44] R. F. Bishop, An overview of coupled cluster theory and its applications in physics, *Theor. Chim. Acta* 80 (1991) 95–148.

- [45] R. F. Bishop, The coupled cluster method, in: J. Navarro, A. Polls (Eds.), *Microscopic Quantum Many-Body Theories and Their Applications*, Lecture Notes in Physics Vol. 510, Springer-Verlag, Berlin, 1998, pp. 1–70.
- [46] C. Zeng, D. J. J. Farnell, R. F. Bishop, An efficient implementation of high-order coupled-cluster techniques applied to quantum magnets, *J. Stat. Phys.* 90 (1998) 327–361.
- [47] D. J. J. Farnell, R. F. Bishop, The coupled cluster method applied to quantum magnetism, in: U. Schollwöck, J. Richter, D. J. J. Farnell, R. F. Bishop (Eds.), *Quantum Magnetism*, Lecture Notes in Physics Vol. 645, Springer-Verlag, Berlin, 2004, pp. 307–348.
- [48] R. F. Bishop, D. J. J. Farnell, S. E. Krüger, J. B. Parkinson, J. Richter, C. Zeng, High-order coupled cluster method calculations for the ground- and excited-state properties of the spin-half XXZ model, *J. Phys.: Condens. Matter* 12 (2000) 6887.
- [49] We use the program package CCCM of D. J. J. Farnell and J. Schulenburg, see <http://www-e.uni-magdeburg.de/jschulen/ccm/index.html>.
- [50] F. Mila, Quantum spin liquids, *Eur. J. Phys.* 21 (2000) 499–510.
- [51] B. Bernu, C. Lhuillier, Spin susceptibility of quantum magnets from high to low temperatures, *Phys. Rev. Lett.* 114 (2015) 057201.